Taylor & Francis
Taylor & Francis Group

Automatika

Journal for Control, Measurement, Electronics, Computing and Communications

ISSN: 0005-1144 (Print) 1848-3380 (Online) Journal homepage: https://www.tandfonline.com/loi/taut20

High-power shortwave DRM transmitter in solid-state technology

Goran Pavlakovic & Silvio Hrabar

To cite this article: Goran Pavlakovic & Silvio Hrabar (2018) High-power shortwave DRM transmitter in solid-state technology, Automatika, 59:2, 158-171, DOI: 10.1080/00051144.2018.1517439

To link to this article: https://doi.org/10.1080/00051144.2018.1517439

Published online: 06 Sep 2018.

AUTOMATIKA
2018, VOL. 59, NO. 2, 158–171
https://doi.org/10.1080/00051144.2018.1517439

REGULAR PAPER

OPEN ACCESS Check for updates

High-power shortwave DRM transmitter in solid-state technology

Goran Pavlakovic[a] and Silvio Hrabar[b]

[a]Transmitter R&D Department, RIZ Transmitter Factory, Zagreb, Croatia; [b]Faculty of Electrical Engineering and Computing, Department of Wireless Communications, University of Zagreb, Zagreb, Croatia

ABSTRACT

Design of high-power shortwave broadcast transmitters is one among the rare areas in the field of radiofrequency (RF) electronics, where the electron tube, as the main element for amplification of RF signal, is still in active use. The first successful attempts to replace the electron tube with solid-state components, primarily in the output stage amplifier modules for the Digital Radio Mondiale (DRM) shortwave broadcast transmitters have been published only recently. With the latest technology advancements in RF power transistors, it is now possible for commercially available RF power MOSFET transistors to be used for switching purposes at shortwave frequencies. Here, an architecture of a 10 kW shortwave broadcast transmitter with solid-state power amplifier modules in the RF output stage is proposed. Different implementations of the RF output stage that include power adding network from each amplifier module and the output matching network are analysed, both analytically and numerically. After choosing the optimal architecture, a prototype of a commercial shortwave DRM broadcast transmitter was designed and constructed, measured, tuned and tested at RIZ Transmitter factory Zagreb.

ARTICLE HISTORY
Received 1 August 2017
Accepted 23 August 2018

KEYWORDS
Radio; transmitter; shortwave; solid-state

1. Introduction

With the advent of electron tube technology in the 1920s, power amplification of electrical signals has played a key function in radio broadcast systems. Those early years of broadcasting offered low efficiency, bulky transmitters. All of the stages inside the early transmitters included vacuum tubes [1]. With the request of lower capital and operational costs, modern shortwave transmitters employ a single electron tube, while the driving amplifier and the modulator unit have been fully transistorized. The electron tube is used only in the output stage, obtaining high-power amplitude-modulated RF signal in the shortwave band (3.9–26.1 MHz) with frequency auto-tuning systems. With the technological improvement in electron tube technology that took place in the late 1980s [2], today's modern shortwave transmitters achieve anode efficiencies up to 83%. This leads to the overall transmitter system efficiencies of more than 70% [3,4]. The single-tube shortwave broadcast transmitter design has been an active field in radio frequency (RF) engineering since the mid-1990s [5–8]. On the other hand, since about 1984, medium-wave broadcast transmitters have turned from the electron tube design to a fully solid-state modular design [9]. This approach offers high overall efficiency ($>85\%$), good audio performance, and higher reliability (there is no inconvenience that occurs when the electron tube fails) [10]. Broadcasting in the shortwave bands, although not as vigorous as before due to the introduction of modern communication technologies (Digital Audio Broadcasting (DAB), Digital Video Broadcasting (DVB), wideband Internet access), still provides an effective means of reaching the distant audience by using high-power shortwave broadcasting systems[11]. An attempt of introducing digital modulation techniques into the shortwave broadcast bands comes in the form of the Digital Radio Mondiale (DRM) standard that introduces Orthogonal Frequency Division Multiplexing (OFDM) modulation techniques in the existing Amplitude Modulation (AM) broadcast bands [12,13]. Using this approach the audio quality on AM bands is the same as in FM bands [14,15]. Modern high-power single-tube shortwave broadcast transmitters are built to accommodate both AM and DRM transmission mode.

Typical architecture of a single-tube shortwave transmitter is shown in Figure 1.

RF exciter generates a carrier signal of precise and stable frequency (within the shortwave frequency range). This low-power signal is further amplified in the driver amplifier, which provides enough power to the control grid of the electron tube. This amplifier is usually a solid-state amplifier operating either in class AB or class B, designed in a push–pull configuration. The necessary impedance transformation from the control grid to the amplifier is utilized using a modified π matching network. A solid-state Pulse Step Modulator (PSM) is used to provide the high-level anode and

CONTACT Goran Pavlakovic goran.pavlakovic@vip.hr Transmitter R&D Department, RIZ Transmitter Factory, Zagreb, Croatia

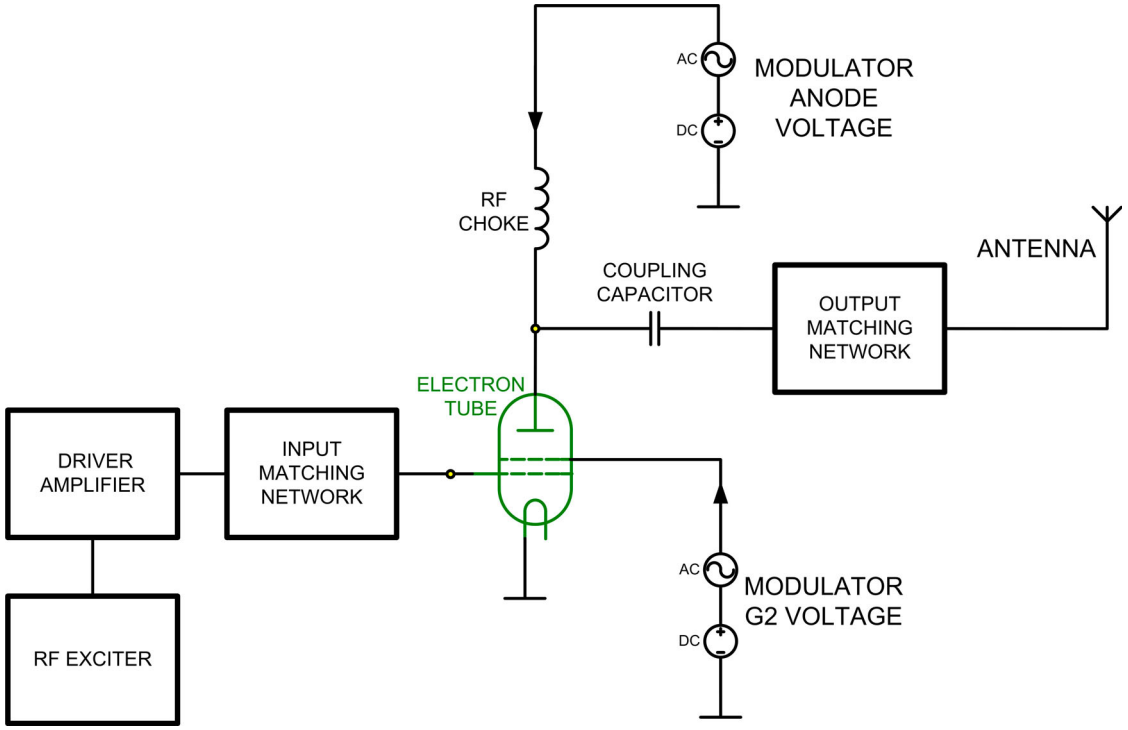

Figure 1. Simplified RF stage of a tube-based modern shortwave broadcast transmitter.

screen grid voltages [16,17]. Modulated RF signal is further brought (via a coupling capacitor) to the output matching network (a triple π configuration). This network provides the necessary impedance transformation and, at the same time, suppresses unwanted harmonic components meeting the specific emissions standard. To provide the necessary digital modulation (OFDM), in-phase and quadrature components of the input signal are converted to polar amplitude and phase components and then applied to the electron tube. Amplitude signal (envelope) is used to modulate the power supply voltages for the anode and screen grid, while the phase signal is used to modulate the control grid of the electron tube. The electron tube is very efficient in the terms of high-power amplification in the shortwave frequency range. However, the electron tube suffers from short lifetime (typically up to 20,000 working hours). Today's solid-state amplifying devices highly surpass this figure, but the possible output power of a single RF transistor is still lower than the output power of a single electron tube.

Up to recent years, due to the technological limitations of RF power transistors, it has not been possible to replace the output stage electron tube with entirely transistorized RF power modules.

Based on our previous experience from the design of fully solid-state (DRM) medium-wave transmitters, we designed and fabricated a power amplifier module suitable for the use at shortwave frequencies, using the currently available commercial RF power transistors. In the following sections, we describe a possible architecture, give an insight in the fabricated RF output stage and present the preliminary experimental results of the prototyped novel shortwave DRM broadcast transmitter in solid-state technology.

2. Basic architecture of high-power shortwave transmitter

The block diagram of proposed high-power shortwave transmitter is sketched in Figure 2. It comprises several power amplifier modules driven from single RF exciter. The output signals from PA modules are combined in the power combiner network, output of which is connected to the output matching network. The purpose of the matching network is twofold: necessary impedance transformation and suppression of unwanted harmonic signals.

RF exciter is capable of generating a dedicated pair of signals which are used to drive each of the power amplifier modules [18]. A special type of power amplifier module with both high efficiency and reliability was designed, manufactured and tested. The details of this module are described in the following section.

3. Power amplifier module

The power amplifier (PA) module, with its principle arrangement shown in Figure 3, is a full-bridge class D type [19]. It consists of four MOSFET transistors that act as controllable switches. A series resonant LC circuit together with the resistive load R are connected to the output of the PA module. By appropriate switching of four transistors, three different voltage levels across the RLC circuit (voltage U_{AB}) are possible. Specifically, when T1 and T3 are in ON state, and T2 and T4 are

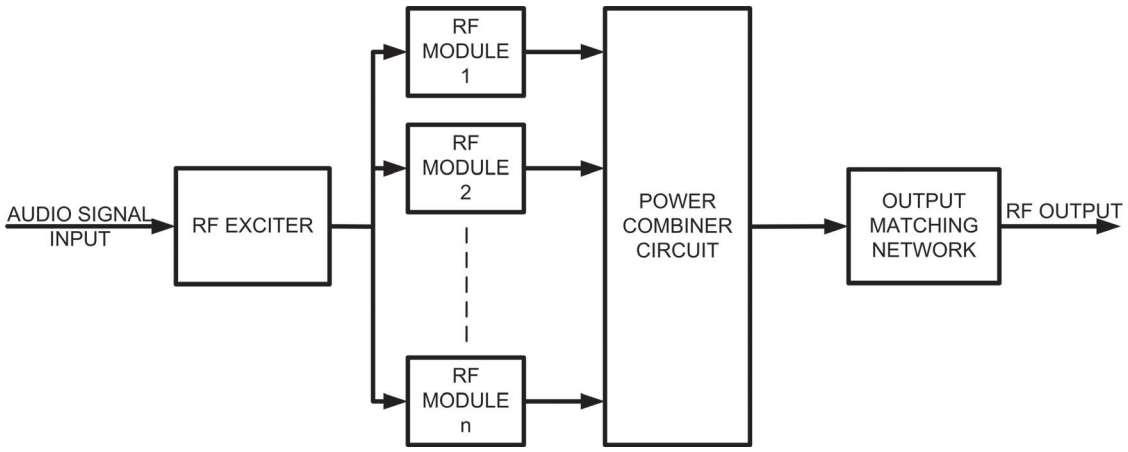

Figure 2. Block diagram of the proposed SW transmitter.

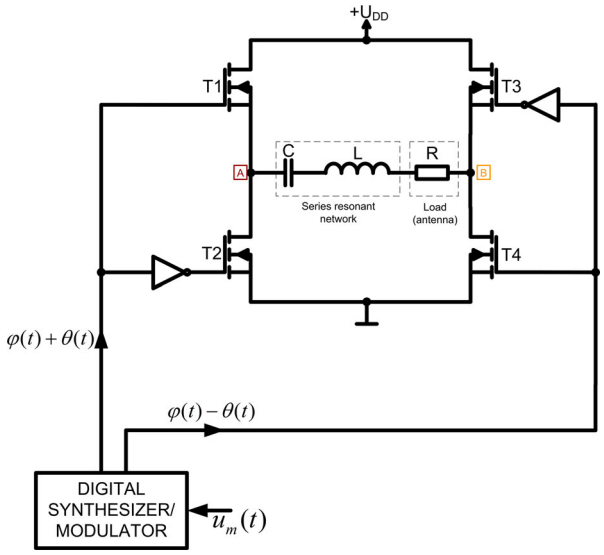

Figure 3. Principle arrangement of class D PA module for shortwave transmitter.

in OFF state, the voltage across the RLC circuit is 0V. The same is valid when T1 and T3 are OFF, and T2 and T4 are ON. When T1 and T4 are ON, and T2 and T3 are OFF, the voltage drop across the RLC circuit is + VDD. When T1 and T4 are OFF, and T2 and T3 are ON the voltage drop across the RLC circuit is – VDD. Thus, adjustment of four controlling signals at the transistor gates it is possible to modulate the width and duty cycle of rectangular waveform signal across the RLC circuit (voltage U_{AB}). It is assumed that the circuit that drives transistors T1–T4 is wideband enough that the frequency of control signals spans across the whole shortwave frequency band. The impedance matching network between the driving circuit and the transistor gate is implemented as a wideband circuit and does not need to be tuned when changing the operating frequency. ARF1511 device – four RF power MOSFETs in one package from Microsemi has been chosen as an adequate switching element for our application. This full-bridge configuration has a 500 V drain–source breakdown voltage and maximum 20 A of continuous drain current with rise and fall time less than 10 ns. The necessary output impedance for the PA module should be tuned in such manner that only the fundamental harmonic of the current flows in the load resistance. This makes the magnitude of the impedance (for higher harmonic components of the output current), as high as possible.

Modern shortwave electron tube transmitters include a separate modulator unit that is used to modulate the anode and the screen grid voltage of the output stage electron tube. On the other hand, modern solid-state modulators are designed as a series chain of lower voltage power supplies, switched on/off according to the input audio signal, thus acting as a very large D/A converter [20,21].

In our case, a different modulation principle is applied. Based on our experience in the medium-wave transmitter design, our intention was to avoid modulation of transistor DC power supply voltage. This has been achieved using the previously described PA module and by utilizing an idea that is based on a modulation principle originally called outphasing, proposed by Henry Chireix in 1935. [22]. Using this principle, it is not necessary to have an additional modulation circuit that modulates the power supply voltage of each transistor. On the other hand, both amplitude and phase modulation are achieved using only phase modulation of the driving signal pair. It is a unique and ingenious method of obtaining the AM signal by the use of a phase modulation and vector addition of two separate radio frequency signals. This basic idea of this modulation method is explained in Figure 4 and in (1)–(7).

An amplitude and phase modulated RF carrier signal can be written in the following form:

$$s(t) = A(t)\cos(\omega_c t + \varphi(t)) \tag{1}$$

Decomposing this signal into two signals of the equal amplitudes one gets:

$$s(t) = s_1(t) + s_2(t) \tag{2}$$

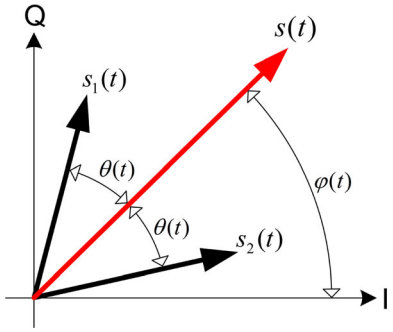

Figure 4. The outphasing modulation concept.

$$s_1(t) = \frac{1}{2} A_m \cos[\omega_c t + \varphi(t) + \theta(t)] \tag{3}$$

$$s_2(t) = \frac{1}{2} A_m \cos[\omega_c t + \varphi(t) - \theta(t)] \tag{4}$$

The outphasing angle is defined as:

$$\theta(t) = \arccos \frac{A(t)}{A_m} \tag{5}$$

In practice, two RF signals $s_1(t)$, $s_2(t)$ are synthesized from a common excitation source. At first, the original signal is split into two separate channels. Signal in each channel is shifted in phase (a positive shift in the first channel and a negative shift in the second channel). Then, the phase of these two signals is modulated by the modulating signal (again, with positive polarity in the first channel and negative polarity in the second channel). The two channels are amplified and then recombined in a vector additive network, which produces the desired modulation type. The main advantage of this type of modulation is high operating efficiency. The two independent channels contain only phase modulated RF signals and therefore each can be amplified to the desired power levels in high efficiency class C or class D amplifiers.

Using quadrature representation of the modulated signal $s(t)$ [23], amplitude and phase components of the modulated signal can be written:

$$A(t) = \sqrt{[I(t)]^2 + [Q(t)]^2} \tag{6}$$

$$\varphi(t) = \arctan\left(\frac{Q(t)}{I(t)}\right) \tag{7}$$

Here $I(t)$ and $Q(t)$ stand for the in-phase and quadrature component of the signal $s(t)$, respectively. In our case, modulation scheme is implemented by applying a phase control of full-bridge class D PA [24]. As shown in Figure 3, audio frequency input modulation signal $u_m(t)$ is processed in a digital synthesizer and converted to a phase change signal and then taken to the gates of each transistor. As explained above, the change in gate-to-drain voltage phase between the pair T1, T2 and pair T3, T4 causes a change in the output voltage duty cycle, therefore changing the amplitude of the carrier voltage and current that flows through the resistive load R. Selection of the full-bridge resistive load was done in three steps and was found to be a value of 20 Ω. In the first step, we selected the full-bridge DC power supply voltage. Based on the maximum drain–source voltage of 500 V, a power supply voltage of 280 V was chosen to accommodate drain–source voltage overshoots that can be caused by inappropriate loading (high VSWR antenna) or improper tuning of output matching network elements.

In the next step we selected the nominal average RF carrier output power. A value of 630 W per power amplifier module was chosen. This value was taken on economic grounds to make the PA module design cost effective.

With the values of the DC power supply and output power selected, we can calculate the resistive load using the following expression:

$$R_{\text{load}} = \frac{U_{AM\_0}^2}{2P_{\text{carr}}} \tag{8}$$

Here P_{carr} is the nominal average output power, U_{AM_0} is the peak voltage of AM carrier signal that can be expressed as:

$$U_{AM\_0} = \frac{\frac{4}{\pi} U_{DD}}{1 + m_a} \tag{9}$$

Here $\frac{4}{\pi} U_{DD}$ is the amplitude of the fundamental harmonic component of the square wave signal with full modulation applied, U_{DD} drain–source DC power supply voltage, m_a is the AM modulation index.

In the third step, transistor RMS drain current was calculated using the following expression:

$$I_{\text{drain}} = \sqrt{\frac{P_{\text{carr}}}{R_{\text{load}}}} \tag{10}$$

In our case this gives a drain current RMS value of 5.6 A well below the maximum continuous drain current. This selection of drain voltage and full-bridge resistive load gives an adequate reserve for stable and reliable long-term operation.

The resulting voltage and current signal waveforms are shown in Figure 5.

Experimental setup that was used for measuring the PA module characteristics is shown in Figure 6. Series RLC circuit in the full-bridge diagonal shown in Figure 3 was replaced with a combination of ferrite core coupled transformer and an impedance matching network. This network was then connected to a commercially available 50 Ω dummy load. Inductance and capacitance values were calculated using the well-known analytical expressions for design of narrowband impedance matching networks. These expressions arise from the quality factor Q, where unloaded quality factors of simple LC networks are used to calculate the

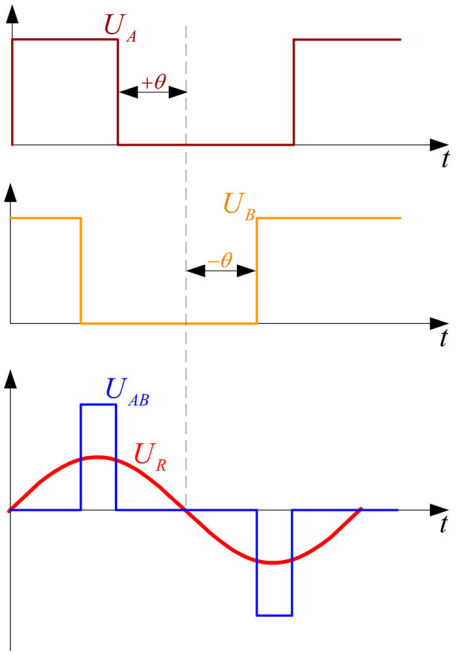

Figure 5. RF PA module drain to source voltages (U_A and U_B for T2 and T4) and the outphasing angle Θ on the upper graph, lower graph shows the diagonal voltage U_{AB} and the load voltage waveform U_R.

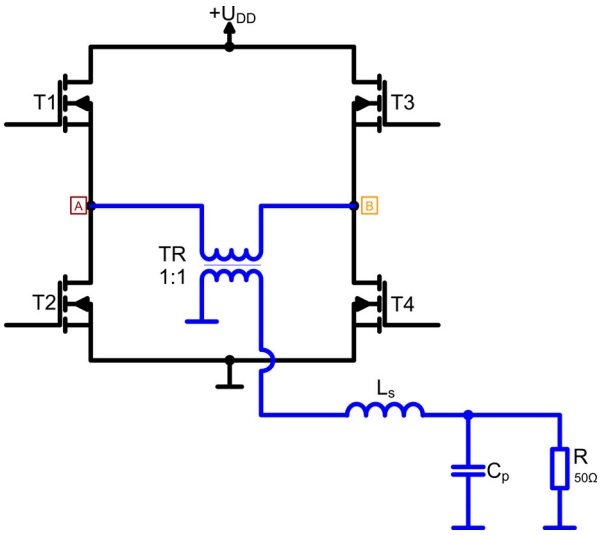

Figure 6. Experimental arrangement of class D PA module for testing and measurements.

impedance transformation between two purely resistive impedance values [25]. Inductance L_s was calculated to be in the range from 0.39 to 1.3 μH, capacitance C_p in the range from 390 to 1300 pF.

A sample of waveform measurements on the prototyped PA module is shown in Figure 7. One can notice that the drain–source voltage is practically a square waveform and the resistive load voltage is a nearly sinusoidal waveform.

The measurements revealed that the PA module is capable of supplying a maximum of 1.0 kW average power to a matched 50 Ω dummy load. Overall PA module efficiency for the nominal carrier power ranges

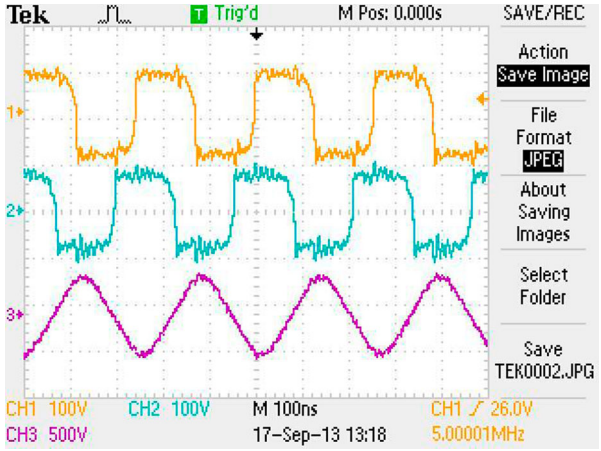

Figure 7. RF PA module voltage and current waveforms. The top trace depicts transistor T2 drain-to-source voltage. The middle trace depicts transistor T4 drain-to-source voltage. The bottom trace depicts the current that flows in the full-bridge diagonal. The measurements were taken at the frequency of 5 MHz).

from 90% at 3 MHz to 85% at 10 MHz that was the highest operating frequency of the manufactured PA module prototype.

4. Power combiner and output matching circuit

Usual means of power combing at RF level include series, parallel or a combination of series and parallel techniques. Usual combining technique in medium wave transmitters employs a ferrite-core-transformer-coupled series combiner, as shown in Figure 8. One can notice that the secondary winding is arranged as a single metal conductor that passes through the centre of all of the ferrite cores. This configuration lowers the values of parasitic elements between the primary and

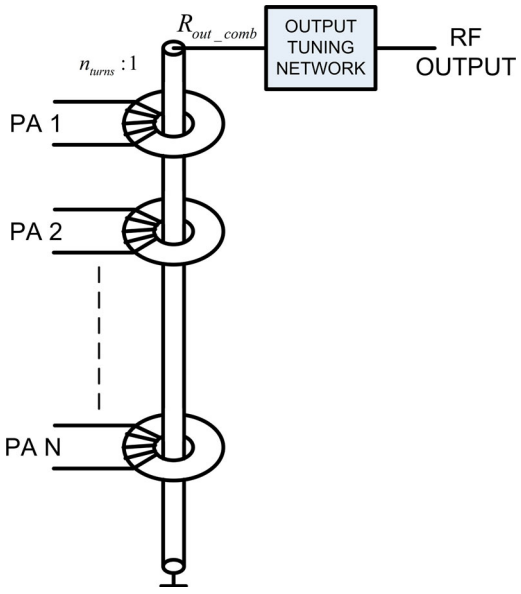

Figure 8. Ferrite core transformer series power combiner.

the secondary transformer winding and it is suitable for high-frequency design.

Choice of the transformer turns ratio depends on the following: impedance transformation ratio between the primary and the secondary and allowable power loss in the core magnetic material. Transformer core magnetic flux density, for a square wave signal, can be obtained using the well-known expression:

$$B_{\max} = \frac{U_{av}}{4A_{ef}Nf}, \tag{11}$$

where $B_{\max}$ is peak AC flux density, U_{av} average AC voltage per half-cycle, A_{ef} effective cross-sectional area, N number of turns, f frequency.

For a given voltage on the primary winding, there is a minimum number of turns on the primary that will not produce overheating of the core. For commercially available ferrite cores, core power losses in dependence on magnetic flux density are given by the manufacturer.

We have addressed the two limitations of this power combiner. First, maximum RF power throughput is limited by the choice of commercially available ferrite cores.

Secondly, usable frequency range of this combiner type is limited by the parasitic inductance and capacitance. Therefore, for a large number of modules connected in series, this design becomes not feasible in practice.

The other function that the series transformer combiner network exhibits is a signal transformation from balanced mode to unbalanced mode. This is especially useful for connecting the full-bridge class D PA module output, which provides an inherently balanced signal, to an unbalanced circuit. The ferrite core transformer primary side can be left open to accommodate the balanced signal on the PA module output, while the secondary side can have one terminal connected to ground, therefore transforming the signal to unbalanced mode that will be suitable for the use in common unbalanced (grounded) circuit topologies.

In the following paragraph, we examine the possible PA module failure effect on the remaining operating PA modules. This is done by investigation of the total output power and the VSWR at the output of each remaining PA module, depending on the number of failed power modules in the combiner. The analysis uses ideal transformer equations and assumes that the failed module is replaced with a short circuit that ensures regular operating conditions of the series combiner network. If the primary is to be left open in the case of PA module failure, then high voltage will be generated at the primary so it is imperative that the primary winding is short circuited in case of PA module failure. This can be done using an additional switching element that will short circuit the failed PA module primary winding. Using the ideal transformer equation it can be shown that the equivalent load impedance at the primary winding is given by:

$$R_{inPA} = n_{\text{turns}}^2 \frac{R_{out\_comb}}{N} \tag{12}$$

The ratio of the combiner output power when all the PA modules are operating and the combiner output power with I modules failed (failed modules replaced with short circuit) is:

$$\frac{P_N}{P_{N-I}} = \left(\frac{N-I}{N}\right)^2 \tag{13}$$

In that case, the corresponding VSWR at the output of each PA module is:

$$\text{VSWR}_{N-I} = \frac{N}{N-I} \tag{14}$$

Inspection of (13–14) shows that the higher the number of PA modules in series the less impact has the failure of PA modules on the output power and the VSWR of each remaining operating PA module. This can be seen in Figures 9 and 10. It can be seen that the influence of failed PA modules on the remaining PA modules in terms of VSWR decreases as the total number of PA modules in the series combiner increases. Although the effect exists, it can be tolerated by the PA module to an extent where the transistor operating values are still located in the safe operating area.

Another technique that can be employed in the shortwave frequency range uses a parallel power combiner. Standard Wilkinson power combiner uses transmission lines and isolation resistors (reject loads) to provide effective matching and isolation at all ports [26]. But, for the use at shortwave frequencies, the length of the transmission lines included in this power combiner type limits its use due to practical reasons. L-C lumped components sections can be used to approximate transmission line sections in the Wilkinson power combiner as shown in Figure 11.

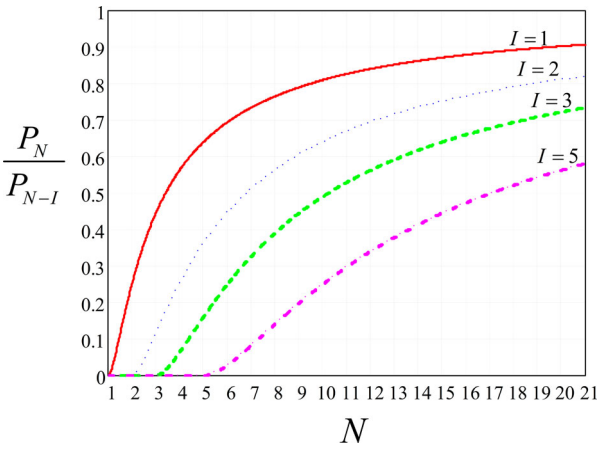

Figure 9. Series combiner output power ratio when I out of N PA modules have failed.

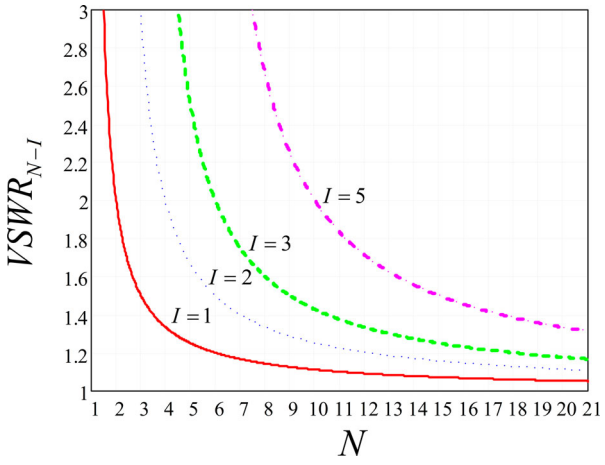

Figure 10. Series combiner VSWR at output of each remaining PA module when I out of N PA modules have failed.

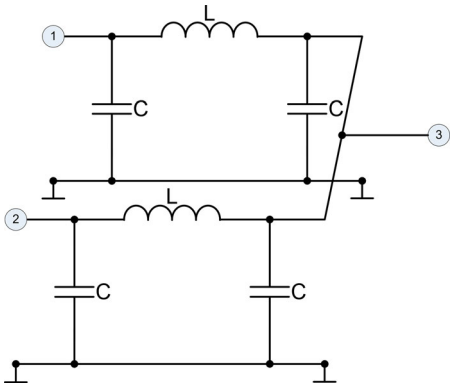

Figure 11. Lumped elements representation of a Wilkinson power combiner.

The lumped elements T section or a π section can be used to replace transmission lines and to provide impedance matching to the next transmitter stage [25]. These matching circuits are inherently narrowband and should include adjustable components to cover the whole shortwave frequency range. Design task for the power combiner and the output matching network is to provide each PA module the necessary impedance at carrier frequency. At the same time, it should obtain a high value of impedance magnitude for all harmonic components at the output of each PA module. The tuning response of each element in the combiner and output matching network on the module impedance should be examined, and the optimum elements for manual and automatic tuning selected.

The simplest lumped elements section that can be used to construct a parallel combiner network is an L section comprised of only two elements (Figure 12). Each of the L sections transforms the PA module output impedance to a higher impedance value. Output from each L section is connected to a common point, where the output impedances of each L section are summed in a parallel manner. Thus, the impedance at the output of the power combiner serves as input impedance

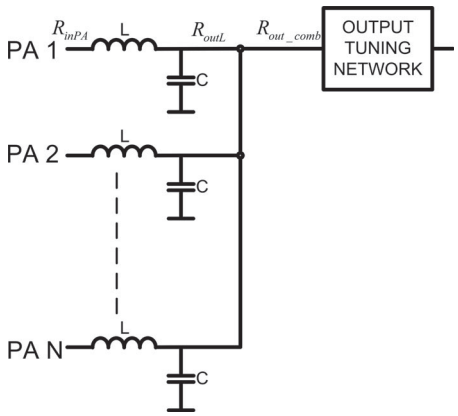

Figure 12. Proposed parallel combiner for shortwave transmitter.

for the following transmitter stage (the output matching network).

One can notice that this parallel combiner contains no isolation resistor networks. They have been omitted with the goal of simplifying the network not just electrically but also economically. Thus, if one of the PA modules fails, the remaining operating PA modules will operate into a detuned load. In practice, this imperfection can be tolerated to some extent where the transistor operating values are still located in the safe operating area. In the case of PA module failure as a short circuit, the impedance added to the summing point node is one of a nearly tuned parallel resonant network L-C. When the PA module fails as an open circuit, only the capacitance C is added to the summing point node and has more influence on the remaining PA modules impedance. Therefore, it is better to short circuit the input of parallel combiner in case of PA module failure. We have also analysed the effect of failed PA module on the impedance of the remaining PA modules for the parallel power combiner (Figure 12). In the practical design the capacitors in the parallel branch can be seen as a single capacitor battery.

Using the Q matching technique the values of the necessary inductance and capacitance can be determined as:

$$Q = \sqrt{\frac{R_{\text{outL}}}{R_{\text{inPA}}} - 1} = \frac{\omega L}{R_{\text{inPA}}} = \frac{R_{\text{outL}}}{\frac{1}{\omega C}} \tag{15}$$

Here, Q stands for quality factor while R_{outL} and R_{inPA} are the output resistance of the L network and the input resistance of the PA module, respectively. The output value of a single L network resistance is:

$$R_{\text{outL}} = NR_{\text{out\_comb}} \tag{16}$$

In the above equation, $R_{\text{out\_comb}}$ stands for the output resistance of the combining network. Analysing the $N-1$ mode failure for the proposed parallel combiner when the failed input is short circuited, one finds the

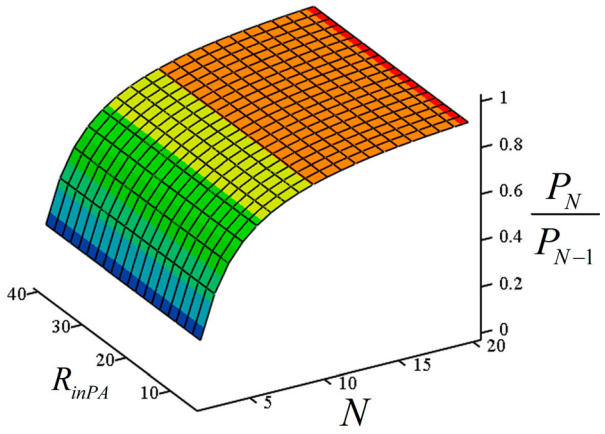

Figure 13. Parallel combiner output power ratio when 1 out of N PA modules has failed.

output power and VSWR for the remaining modules as shown in Figures 13 and 14, respectively.

The combining network is connected to the output matching network. It can be realized as a standard L, T or π matching network, or as a combination of these networks. It should meet the following requirements. First, it needs to obtain the necessary impedance transformation between the transmitter output and the combiner output. Second, it needs to ensure sufficient attenuation of harmonic signals at the transmitter output that will meet the regulatory emission standards. Third, in the case of transmitter load mismatch, caused by antenna or transmission line impedance variation up to a certain VSWR level, it should be able to tune the transmitter output to its nominal power.

For the implementation of a prototype transmitter we have chosen an output matching network that consists of a T matching section as shown in Figure 15. Capacitor C and inductor L2 have been chosen for manual or automatic tuning that covers the variations of the output transmitter load.

Analysed combiner and output matching networks contained idealized elements. Of course, in practice, these elements will include parasitic components that

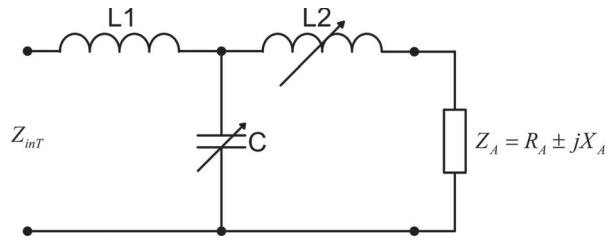

Figure 15. T section output tuning network (Z_A stands for antenna impedance).

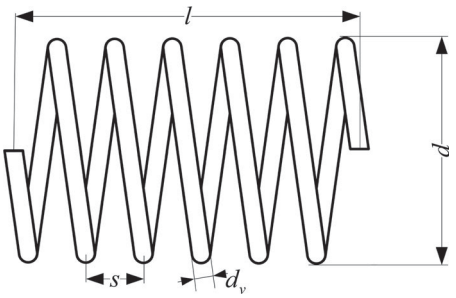

Figure 16. Single-layer helical round wire coil inductor.

will disturb the idealized circuit behaviour, especially at higher harmonic components frequencies. To take these effects, that are of the electromagnetic nature, into account, it is necessary for the circuit model to include the wideband models of real inductors and capacitors. A commercial numerical electromagnetic simulator CST^{TM} has been used to characterize and to optimize the wideband frequency behaviour of the real inductors, while for the real capacitor a well-known model that describes its behaviour at higher frequencies was used.

To achieve the desired inductance in real shortwave high-power transmitter applications, inductors wound with copper wire or tubing are frequently used. One inductor type, a single-layer helical round wire coil is shown in Figure 16.

One of the oldest, but still very frequently used empirical expression for the inductance was given by

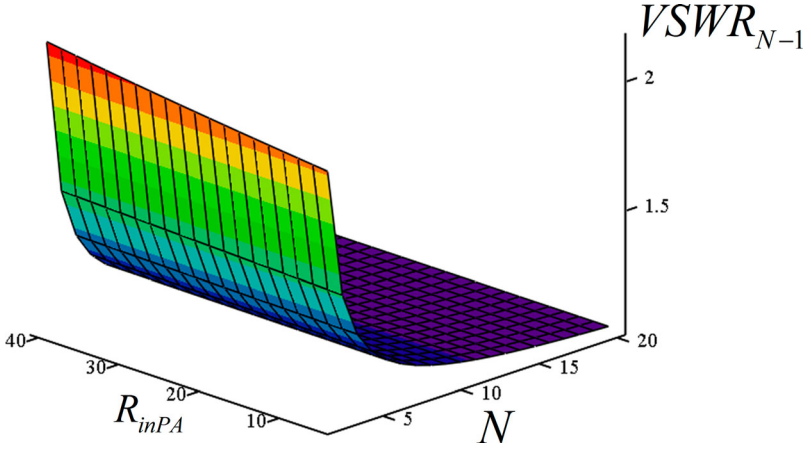

Figure 14. Series combiner VSWR at output of each remaining PA module when 1 out of N PA modules has failed.

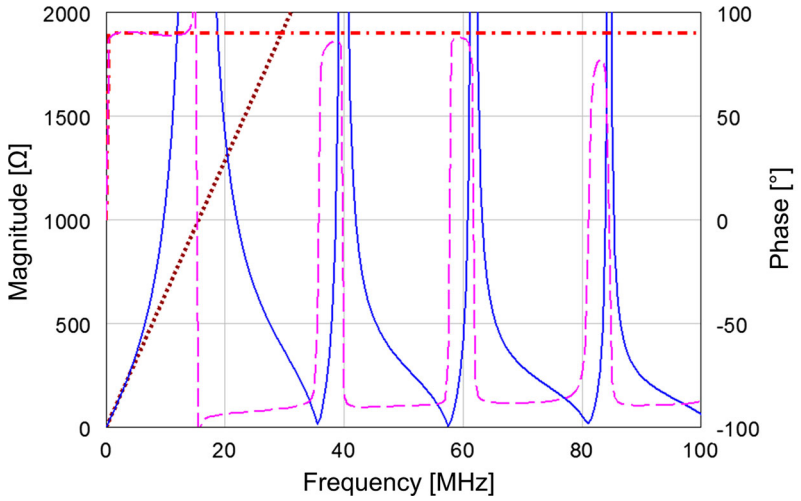

Figure 17. Impedance of a helically wound inductor shorted on one end (magnitude solid line, phase dashed line) compared to an ideal lumped inductor (magnitude dotted line, phase dash-dot line).

H.A. Wheeler [27]:

$$L = \frac{d^2 N^2}{l + 0.45d}. \tag{17}$$

The above formula is valid only as a lumped element approximation, while because of its electromagnetic nature, the frequency behaviour of this structure is complex and includes describing the coil as a helical waveguide [28]. A numerical analysis of this electromagnetic structure shows that it behaves as an ideal lumped inductor only in the frequency range where there is no change of the phase of the magnetic field across the device as stated by the circuit theory. Above this frequency range its behaviour resembles one of a short-circuited transmission line.

Yet another property of the inductor is its power handling ability. In general, high-power circuit elements, due to demand for efficient cooling, should have certain mechanical dimensions. This implies that their high-frequency behaviour will no longer be of lumped nature. While for the carrier frequency elements can be modeled as lumped, for the higher harmonic components this is no longer valid. Figure 17 shows the impedance (magnitude and phase) of a helical coil short circuited on one end. These results have been obtained from a numerical electromagnetic simulation (using CST^{TM} software) of a coil with the following dimensions: $d = 200$ mm, $l = 300$ mm, $s = 30$ mm, $N = 10$, $dv = 10$ mm. For comparison, magnitude and phase of a lumped inductor are also drawn. The inductance value of the lumped inductor is calculated by (17) with the above-stated coil dimensions.

One approach that is useful to avoid numerical simulations is to describe the helically wound coil as a transmission line. In their work, Corum and Corum give the expression for the frequency dependent characteristic impedance that can be used to model the coil as a transmission line in electronic circuit simulators [29]. Shortwave transmitter output stage is a low-volume, high-power surrounding so it is important to determine the power dissipation of each element to provide sufficient cooling. The coil structure losses can be characterized by the skin and proximity effect, as done by Medhurst empirically [30] or by numerical techniques. A numerical analysis of the coil structure loss caused by high-frequency surface currents is shown in Figure 18. The simulation (using commercial CST^{TM} software) has been done for the coil of above-stated dimensions with 15 kW of average RF power applied to a series coil-to-load combination. It can be seen that the power loss appears on the inner surface of the copper tubing looking towards the centre axial axis of the coil, because the majority of the RF current flows in this area.

Capacitors that are commonly used in high-power transmitters have vacuum as the dielectric between the electrode plates [31]. They can be either of fixed capacitance or variable capacitance as shown in Figure 19.

This capacitor structure is usually modelled by the simple circuit schematic shown in Figure 20. The parallel resistance (R_{EPR}) represents the dielectric losses while the series resistance (R_{ESR}) represents losses caused by skin-effect. L_s is the parasitic inductance connected in series with the capacitance. Values of these parasitic components are stated in the vacuum capacitor manufacturer's datasheets [32].

Taking into consideration the effects of real inductors and capacitors and optimizing their design with the goal of minimizing the influence of parasitic components, results in the final form of the RF output stage for a 10 kW prototype transmitter. The combiner circuit and the output matching network form a new circuit as shown in Figure 21.

Based on our analysis we have chosen three PA modules to be combined in series manner and then seven PA module "trios" in parallel manner. This gives the total number of 21 PA modules enough to provide 40 kW of Peak Envelope Power (PEP) power on the transmitter output.

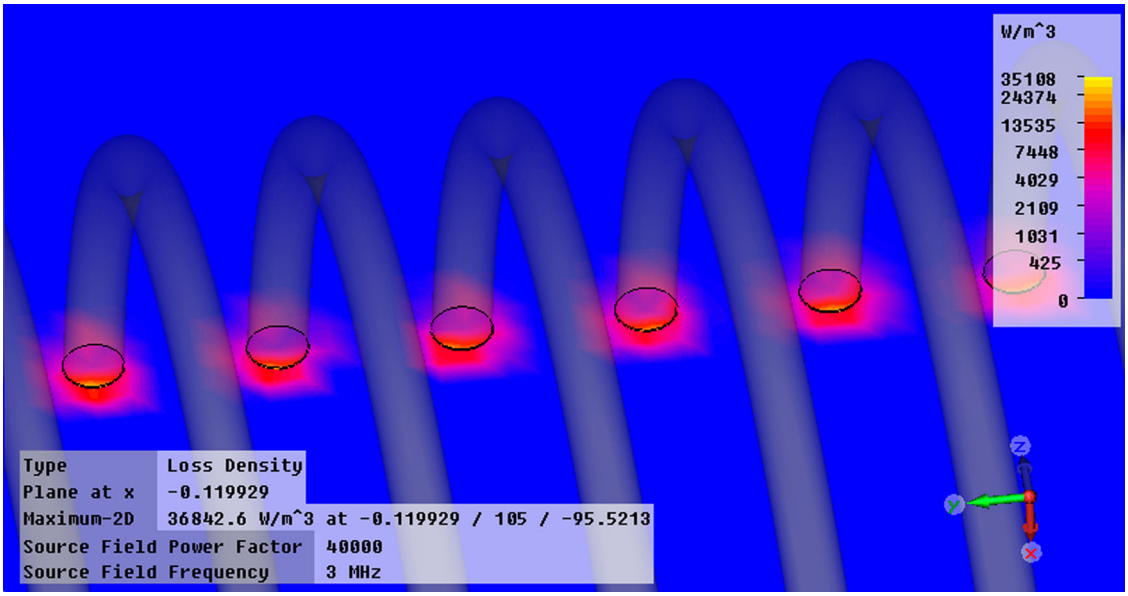

Figure 18. RF power loss density on a helical inductor (simulation using CST^{TM} electromagnetic solver).

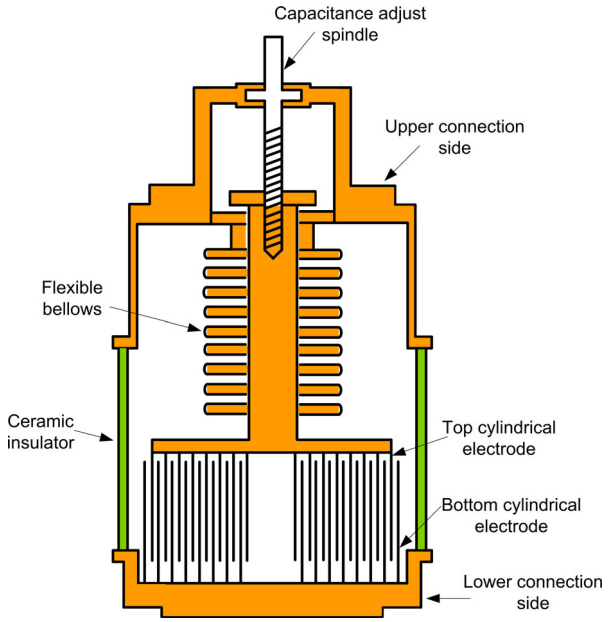

Figure 19. Typical variable vacuum capacitor [31].

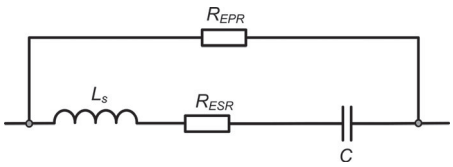

Figure 20. Equivalent capacitor model schematic.

The harmonic signals of each PA module are attenuated through the combiner network and through the output matching network. The PA output signal waveform is a bipolar rectangle voltage with a variable duty cycle (as previously shown in Figure 7). Applying the Fourier transform we find it contains only the odd mode components of the carrier frequency. These harmonic components are filtered out in the power combiner and the output matching network. It obtains the high efficiency of used PA module.

5. Solid-state 10 kW shortwave transmitter prototype

In the previous sections, we have described and analysed all of the elements necessary to construct a novel fully solid-state 10 kW shortwave broadcast transmitter. The physical structure of the prototype transmitter RF output stage is shown in Figure 22. The vacuum capacitors are commercially (COMET Company) while the inductors were in-house designed, optimized and constructed. The design process should satisfy the demands for optimal frequency behaviour and the necessary power handling. Twenty-one PA modules are arranged in a 3×7 configuration, where 3 PA modules are combined in series via ferrite transformer combiner and stacked horizontally. Seven of these are then combined in a parallel manner through the inductors stacked vertically that are connected to a common capacitor battery on their ends. The output matching network is a T section that consists of two separate L sections. This has been done so that voltage and current can be measured at the middle of the T section for proper output load tuning. The initial tuning of elements in the RF output stage, without RF power applied from the output of the PA modules, was done using a vector network analyser observing the matching elements impedance.

The transmitter output was then connected to a dummy load and tuned. Voltage and current waveforms at PA module output were measured and can be seen in Figures 23 and 24. Higher operating frequency currents show the existence of not only the carrier frequency but also harmonic components that are caused by the non-ideal behaviour of the RF output

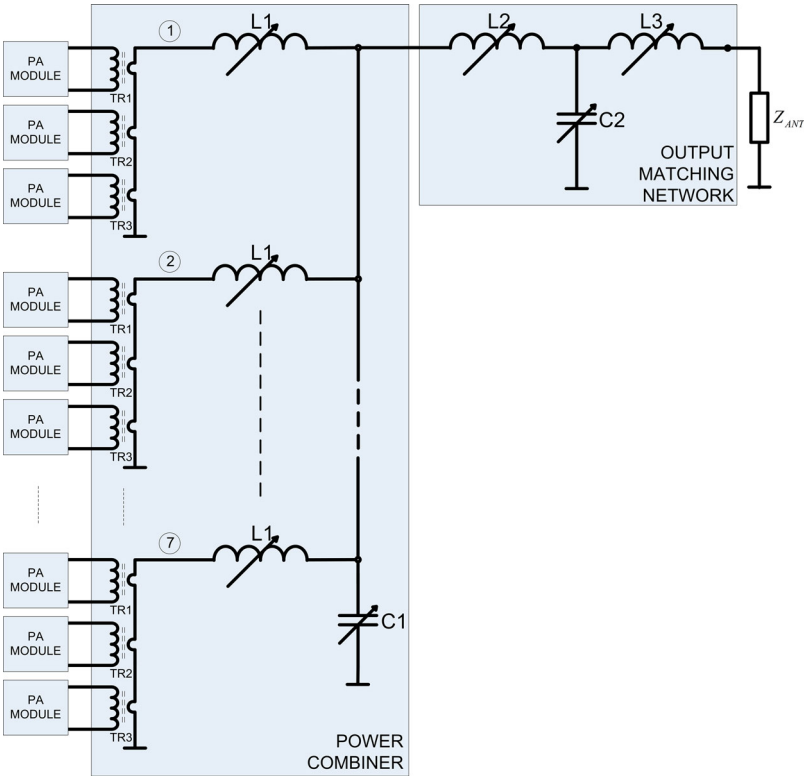

Figure 21. Final combiner circuit and the output matching network form the RF output stage.

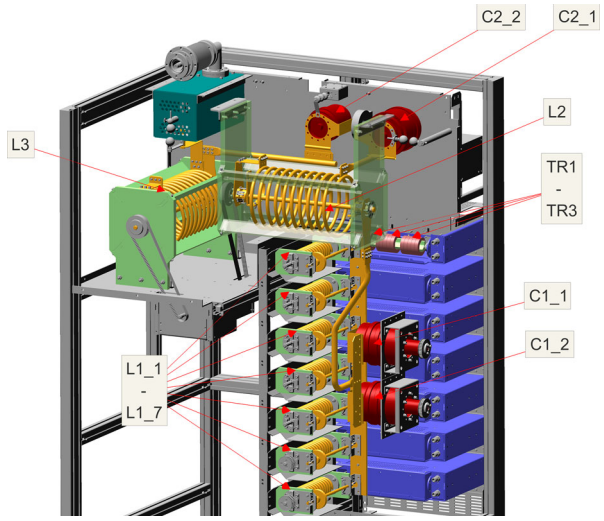

Figure 22. RF output stage layout inside the transmitter prototype.

stage elements. These harmonic components produce additional power dissipation in the RF output stage components. Measured RF system efficiency, ratio of average RF output power and PA modules input DC power, for RF carrier conditions without modulation applied, was from 65 to 75% depending on the frequency (smaller value for higher operating frequencies). With AM modulation applied, values from 70% to 80% were measured. In DRM mode, RF system efficiency values of 55–65% were measured. Observing the RF circuit, power is being dissipated mainly in the transistors due to switching losses, in the combiner transformer cores, and in lesser amount in the RF output stage inductors, capacitors and copper conductors. Overall transmitter efficiency, ratio of average RF output power and input AC power that includes all transmitter losses and auxiliary systems consumption, was found to be in the range from 60% to 70% in AM mode, 50–60% in DRM mode.

Cooling system includes forced water cooling of the PA module and natural convection cooling of inductors and capacitors in the RF output stage. A maximum temperature increase of 25°C, relative to ambient temperature, was registered on the surfaces of RF output stage elements when operating the transmitter at 40 kW peak envelope RF power with modulation applied.

Figure 25 shows a spectrum of the transmitter output signal when operating in DRM mode. The output signal spectrum satisfies the standard spectrum mask for DRM transmission. DRM, as mentioned in the introduction, is a technology that uses OFDM modulation technique in the existing AM broadcast bands. The modulation bandwidth depends on the broadcast robustness mode and can be from 4.5 to 20 kHz. Peak-to-average power ratio of DRM signal can attain a value of 12 dB, but in the transmitter design it is usually decreased to 9 dB using peak-to-average power ratio reduction techniques. Adaptive linearization with polynomial amplitude and phase predistortion functions was used to linearize the power amplifier. In the RF Exciter, adaptive digital predistortion was implemented in FPGA technology. Feedback signal from the TX output is taken to the RF exciter where it is used by the linearization algorithm to train the predistortion filter

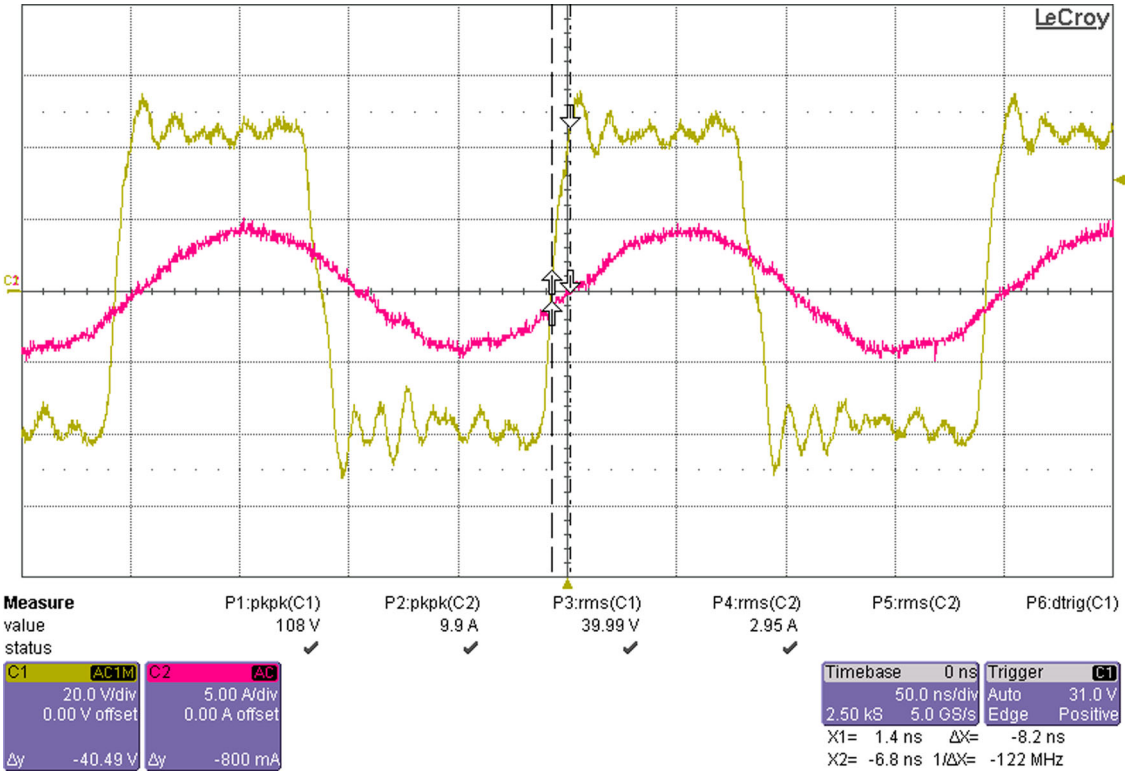

Figure 23. Voltage (square-like) and current (sine-like) waveforms observed at PA module output at 5.020 MHz.

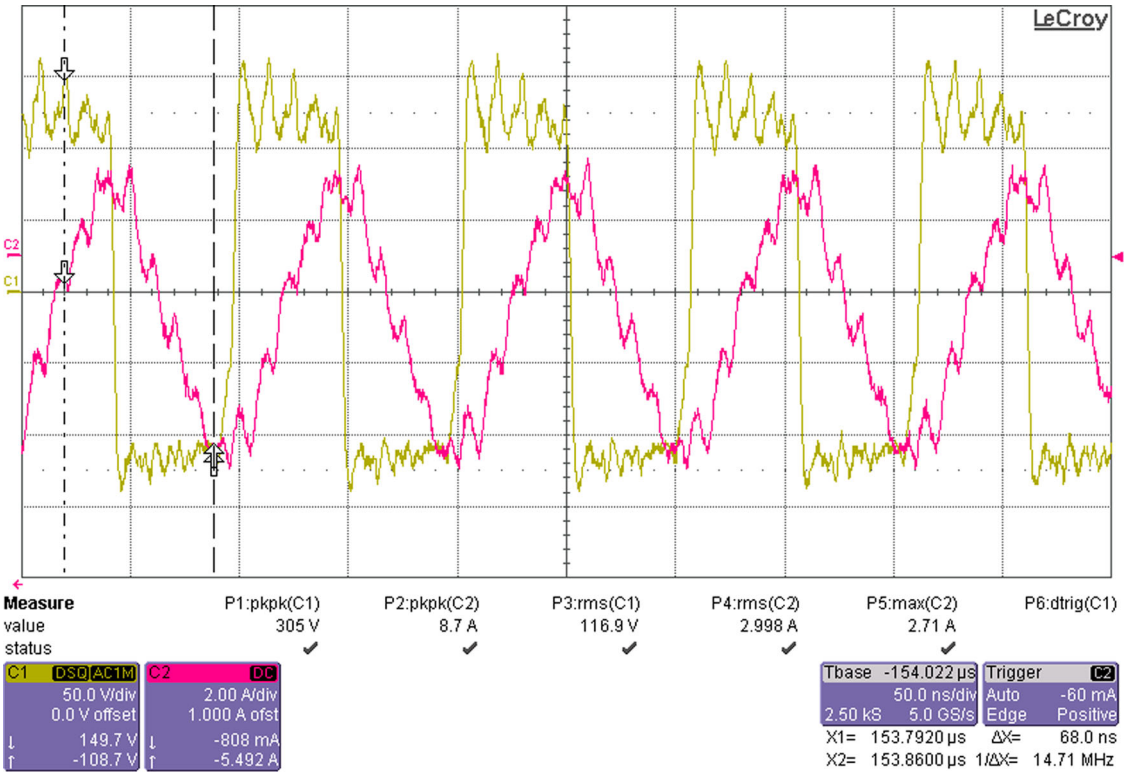

Figure 24. Voltage (square-like) and current (sine-like) waveforms observed at PA module output at 9.545 MHz.

polynomial coefficients that are stored in a look-up table (LUT).

6. Conclusions

A concept of a new fully solid-state shortwave transmitter has been presented. A practical design of a class D power amplifier module that is a basic building block for the new shortwave transmitter, has been shown and experimentally verified. Possible series and parallel combining techniques for the shortwave PA modules have been studied. The combiner network includes a combination of series and parallel combining techniques. The series combiner uses RF transformers

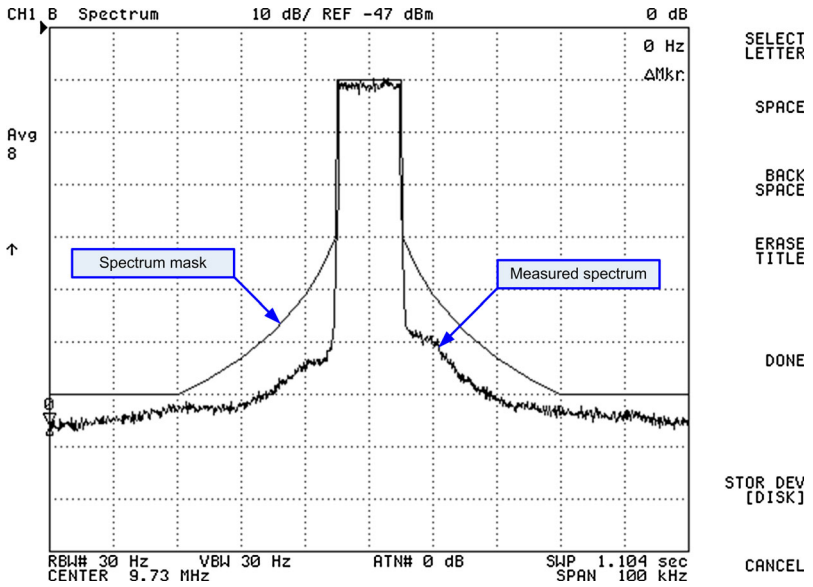

Figure 25. Measured spectrum of the transmitter output signal when operating in DRM mode.

with ferrite cores with secondary winding connected in series, while the parallel combiner uses L matching circuits connected in parallel. Wideband frequency behaviour of real inductors and capacitors has been considered and taken into account for the design of a complete RF output stage that includes the PA modules, combiner and output matching network. In the next step, prototype of a fully solid-state shortwave transmitter was designed and constructed. Measurements were carried out and the results have revealed stable operation with 10 kW RF power and overall transmitter efficiency between 60% and 70% in AM, 50% and 60% in DRM mode. Novel solid-state transmitter architecture satisfies all the conditions for transmitter application in commercial shortwave broadcasting. Although the new solid-state transmitter prototype circuits and elements have been designed and optimized with the goal to satisfy lumped theory behaviour, the effects that arise from the electromagnetic nature of real-world inductors and capacitors cannot be avoided, what is true especially when operating at higher carrier frequencies. One of the most critical aspects of the design is how to avoid the existence of harmonic components in the PA module output current and needs to be studied in more detail in the future.

Disclosure statement

No potential conflict of interest was reported by the authors.

References

[1] Fenn RE. The transmitter. EBU Technical Review; 1995.
[2] Mark JT, McNees SG. New high efficiency 500 kW tetrodes for short wave broadcast. IEEE Trans Broadcast. 1988;34(2):141–146.
[3] Schminke W. The merits of modern technology for today's high power short-wave transmitters. IEEE Trans Broadcast. 1988;34(2):126–133.
[4] Tomljenovic J, Tschol W. AM radio transmitter with a final stage tetrode. U.S. Patent No. 5,261,123. 1993 Nov.
[5] Wood J. Developments in the design and performance of HF transmitters. Electron Power. 1987;33(6):392–396.
[6] Mina A, Weldon JO, Hulsey G. An improved high efficiency 500 kilowatt short wave broadcast transmitter with novel features. IEEE Trans Broadcast. 1988;34(2):134–136.
[7] Bingeman GW. Computer control and monitoring of the 420B-1 500 kW HF transmitter. IEEE Trans Broadcast. 1988;34(2):137–140.
[8] Binns JFH, McGann M, Owen EG. The necessary features of high power, HF broadcast transmitters now and in the future. Brighton, UK: International Broadcasting Convention. 1990.
[9] Swanson H. Digital AM transmitters. IEEE Trans Broadcast. 1989;35(2):131–133.
[10] Hubert N. A high power solid-state medium wave broadcast transmitter. IEEE Trans Broadcast. 1989;35(2):118–120.
[11] Wood J. The future of terrestrial broadcasting-the short-wave super transmitter. IEE Rev. 1989;35(4):131–134.
[12] Stott J. Digital radio mondiale: key technical features. Electron Commun Eng J. 2002;14(1):4–14.
[13] Hofmann F, Hansen C, Schafer W. Digital radio mondiale (DRM) digital sound broadcasting in the AM bands. IEEE Trans Broadcast. 2003;49(3):319–328.
[14] Prieto G, Pichel I, Guerra D, et al. Digital radio mondiale: broadcasting and reception. Proceedings of the 12th IEEE Mediterranean Electrotechnical Conference, Dubrovnik, Croatia; 2004. Vol. 2, p. 485–487.
[15] Bradley MJ. Digital radio mondiale: system and receivers. Ninth International Conference on HF Radio Systems and Techniques, Bath, UK (Conf. Publ. No. 493). 2003. p. 198–202.
[16] Wysocki B. PDM transmitters. IBC Proceedings, London, UK. 1978. p. 122–126.
[17] Swanson HA. The Pulse Duration Modulator . . . A new Method of High Level Modulation in Medium and Shortwave Broadcast Transmitters. Gates Engineering Report, Gates Radio, Quincy (IL).

[18] Raab FH, Asbeck P, Cripps S, et al. Power amplifiers and transmitters for RF and microwave. IEEE Trans Microw. Theory Tech. 2002;50(3):814–826.
[19] Kazimierczuk MK. RF power amplifiers. New York, USA: John Wiley and Sons; 2008; p. 152–160.
[20] Bowers DF. Pulsam a new amplitude modulation. Syst Commun Broadcast. 1981;6(3):25–32.
[21] Schminke W. High-power pulse-step modulator for 500kW short-wave and 600kW medium-wave transmitters. Brown Boveri Rev. 1985;72(5):235–240.
[22] Chireix H. High power outphasing modulation. Proc Inst Radio Eng. 1935;23(11):1370.
[23] Haykin S. Communication systems. 4th ed. New York, USA: John Wiley & Sons; 2001; p. 725–730.
[24] Zhang X. Design of linear RF outphasing power amplifiers. Norwood (MA): Artech House; 2003; p. 145–159.
[25] Bahl IJ. Lumped elements for RF and microwave circuits. Norwood (MA): Artech House; 2003; p. 370–377.
[26] Wilkinson EJ. An N-way hybrid power divider. IRE Trans Microwave Theory Tech. 1960;8(1):116–118.
[27] Wheeler HA. Simple inductance formulas for radio coils. Proc. IRE, Menasha, USA. October 1928. p. 1398, and March 1929, p. 580.
[28] Sichak W. Coaxial line with helical inner conductor. Proceedings of the IRE, Menasha, USA. 1954. p. 1315–1319. (Corrections, February, 1955, p. 148.).
[29] Corum KL, Corum JF. RF coils, helical resonators and voltage magnification by coherent spatial modes. 5th International Conference on Telecommunications in Modern Satellite, Cable and Broadcasting Service, Nis, Yugoslavia. 2001, Vol. 1, p. 339–348.
[30] Medhurst RG. H.F. resistance and self-capacitance of single-layer solenoids. Wireless Engineer, February 1947, p. 35, and March 1947, p. 80.
[31] Giers L. Vacuum variable capacitors – an introduction to their design, rating and installation. Cathode Press. 1966;23(4):22–29.
[32] Technical Recommendations and General Instructions for Vacuum Capacitors, Comet AG plasma control technologies. Service Bulletin; 52.